JACS
JOURNAL OF THE AMERICAN CHEMICAL SOCIETY

COMMUNICATION

pubs.acs.org/JACS

Spin Transition Charted in a Fluorophore-Tagged Thermochromic Dinuclear Iron(II) Complex

Yann Garcia,* François Robert, Anil D. Naik, Guangyuan Zhou, Bernard Tinant, Koen Robeyns, Sébastien Michotte, and Luc Piraux

Institute of Condensed Matter and Nanosciences, Université Catholique de Louvain, Place Louis Pasteur 1, 1348 Louvain-la-Neuve, Belgium

Supporting Information

ABSTRACT: The first crystal structures of a dinuclear iron(II) complex with three *N*1,*N*2-1,2,4-triazole bridges in the high-spin and low-spin states are reported. Its sharp spin transition, which was probed using X-ray, calorimetric, magnetic, and ^{57}Fe Mossbauer analyses, is also delineated in the crystalline state by variable-temperature fluorimetry for the first time.

Molecular electronics attained a rapid pace with the influx of some of the finest switchable materials and foresees harvesting them as prospective components in fabricating accessories for information processing, data storage, sensors, etc.[1] Single-molecule magnets (SMMs),[2] quantum dots,[3] thermo-photoelectrochromic materials, and iron(II) spin-crossover (SCO)[1] materials are at the forefront of this race. Not lagging behind, contemporary probing techniques such as optical imaging,[4] atomic force microscopy,[5] transmission electron microscopy,[6] scanning tunneling microscopy,[7] ellipsometry,[8] etc., have inventively provided a wealth of information in support of other routine spectroscopic techniques in probing and understanding the process and dynamics of SCO solids, nanoparticles, liquid crystals, and thin films.[9] The principle that is technologically significant in iron(II) SCO is the possibility of addressing two distinct spin states involving d-electron relocation.[1] Designing a SCO material tagged with a fluorophore that could sense or "feel" the SCO signal ripping through the molecular network and thereby providing an opportunity to register the SCO has been a long-lasting aspiration.[10] Such a protocol would undoubtedly have prospects in the fields of biomarkers, drug delivery, biological imaging, and thermometry.[11] Successful attempts have been made by designing one-dimensional (1D) iron(II) SCO nanoparticles including a fluorescent agent such as rhodamine 110[11] or 3-(dansylamido)propyltrimethoxysilane.[12] However, 1,2,4-triazole derivatives are the best-suited molecular fragments for this purpose,[13] as a fluorophore can be inserted at a remote position (N4) that is unlikely to encounter direct metal ion contact, which otherwise could have a deleterious effect of fluorescence quenching. It could be anticipated that the fluorophore could display optical properties depending on its sensitivities to the diamagnetic low-spin (LS) and paramagnetic high-spin (HS) states of iron(II) ions. This design followed by synthesis led to *N*-salicylidene-4-amino-1,2,4-triazole (**L1**) [see the Supporting Information (SI)], which belongs to the family of photo- and thermochromic anil Schiff bases[14] and was selected because of its strong emission properties in the solid state.[15]

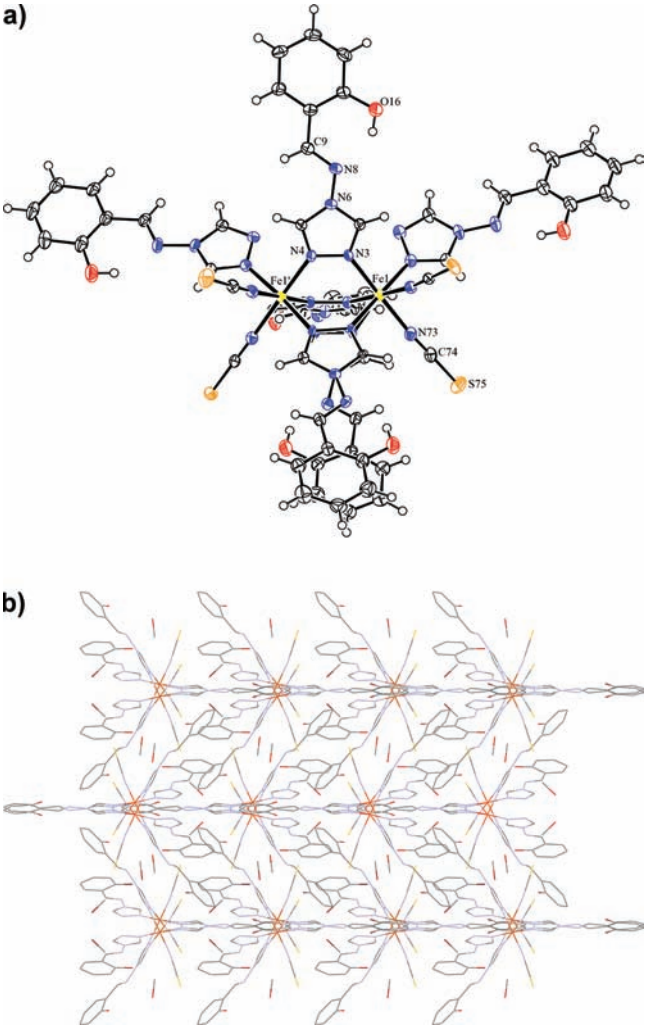

Figure 1. (a) ORTEP view of the asymmetric part of the unit cell of **1**, showing 50% probability displacement ellipsoids. (b) View of the crystal packing along the *a* axis.

Upon reaction of **L1** and $Fe(NCS)_2$ in MeOH under a dry Ar atmosphere, bright-yellow single crystals of the dinuclear complex $[Fe_2(\mathbf{L1})_5(NCS)_4]\cdot 4MeOH$ (**1**) were obtained (see the

Received: June 27, 2011
Published: September 21, 2011

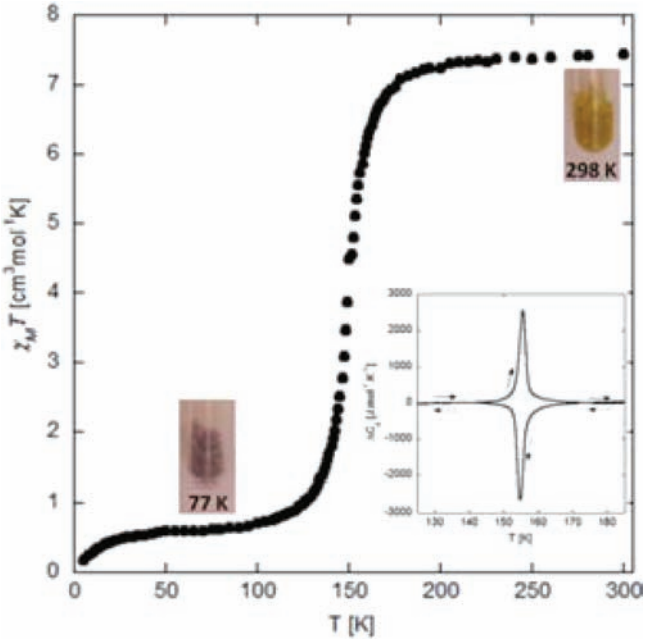

Figure 2. $\chi_M T$ *vs* T plot for **1**. The inset shows both exothermic and endothermic DSC peaks on cooling and warming. Photographs of **1** demonstrate thermochromic properties.

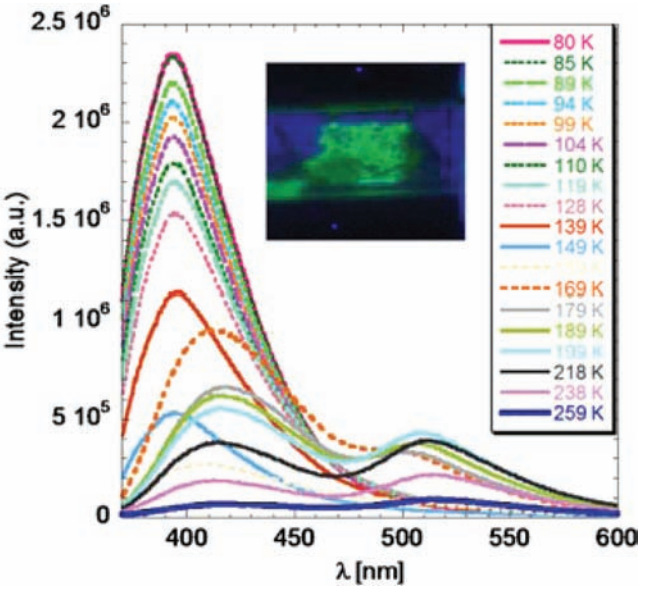

Figure 3. Temperature-dependent emission spectra for **1** at λ^{ex} = 350 nm for T = 80−259 K. The inset shows the fluorescence of **1** at 293 K produced by continuous irradiation at 254 nm.

SI). Crystal structure analysis at 100(2) K showed the monoclinic space group $C2/c$. Crystal data and structural parameters are given in Tables S1 and S2 in the SI. The iron atoms in the dinuclear unit are separated by 3.648(7) Å (Figure 1) and bridged by three bidentate **L1** ligands through N1 and N2 of the 1,2,4-triazole. The octahedral coordination sphere around each iron atom is completed by two *cis*-isothiocyanato anions and one monodentate *N*1-**L1** ligand, affording an FeN_6 environment.

The average Fe−N bond length of 1.983(2) Å is typical of LS iron(II) ions.[1] In the terminal and bridging **L1**, the C−O and C═N bond lengths evidence the enol form of the ligand (Table S2). Indeed, each terminal **L1** presents a strong intramolecular H-bond between the alcohol and the imine functions (Table S3). The third bridging ligand presents a disordered conformation (see the SI). These two significantly different conformations are eased by a dense supramolecular network involving H-bonds and $\pi-\pi$ stacking interactions (Table S4 and Figure 1b). This network also promotes a steep spin transition (ST) curve, which is supported by the absence of any crystallographic phase transition (see Figure 2). Indeed, at 200(2) K, the $C2/c$ space group is retained, and the Fe···Fe distance is stretched to 3.966(8) Å. The drastic increase in the Fe−N bond lengths [avg 2.180(3) Å] is typical for HS iron(II) ions and is a signature of a SCO. Moreover, the enol form of each **L1** is preserved, as shown by the C−O and C═N bond lengths[16] (Table S2).

Magnetic susceptibility data of single crystals of **1** were recorded over the temperature range 300−5 K (Figure 2). At room temperature, the $\chi_M T$ product is 7.46 cm^3 K mol^{-1}, which corresponds to two noncoupled HS iron(II) ions. On cooling, $\chi_M T$ drops abruptly between 161(1) and 138(1) K to 0.60 cm^3 mol^{-1} K, indicating a partly incomplete ST with a transition temperature ($T_{1/2}$) of 150(1) K. The decrease in $\chi_M T$ observed below 50 K is due to zero-field splitting and weak antiferromagnetic coupling of the remaining HS iron(II) ions.[1] The ^{57}Fe Mössbauer spectrum at 77(1) K (Figure S1 in the SI) confirmed the incomplete character of the ST by showing with two quadrupolar doublets, one corresponding to the LS state [isomer shift δ^{LS} = 0.513(1) mm s^{-1} and quadrupole splitting ΔE_Q^{LS} = 0.150(3) mm s^{-1}] with a relative area fraction A^{LS} = 94(2)% and the other to the HS state of the same iron site [δ^{HS} = 1.21(5) mm s^{-1}, ΔE_Q^{HS} = 2.95(9) mm s^{-1}) with A^{HS} = 6(2) % (Table S5). The ST was fully confirmed by Mössbauer spectroscopy on warming, leading to 100% HS species at room temperature and $T_{1/2}$ = 150(1) K, in perfect agreement with the superconducting quantum interference device (SQUID) data (Figure 2). The presence of a single iron site supports a ST mechanism that proceeds in one step from [HS−HS] to [LS−LS] pairs without an intermediate [LS−HS] phase. A first-order phase transition was confirmed by differential scanning calorimetry (DSC) over the ST range with T_{max} = 155(1) K, corresponding well to the $T_{1/2}$ obtained in the SQUID and Mössbauer measurements (Figure 2). The enthalpy and entropy variations[1] associated with the ST are ΔH = 8.6 kJ mol^{-1}, ΔS = 55.5(1) J mol^{-1} K^{-1}, and ΔS_{vib} = 42.1(1) J mol^{-1} K^{-1}.

A crystalline sample of **1** showed a reversible thermochromic effect from bright-yellow at 298 K to deep-burgundy at 77 K (Figure 2 inset), confirming a SCO as **L1** retains its white color down to 77 K.[15] Diffuse reflectance of **1** at room temperature (Figure S2) showed an intense signal at ∼390 nm attributed to the enol form of **L1**[15] along with an intense band centered at ∼410 nm attributed to the *cis*-keto form of **L1** as well as a third broad band from 630 nm to the IR region assigned to a metal-to-ligand charge-transfer transition.

Comparative analysis of variable-temperature fluorescence measurements of crystalline samples of **L1** and **1** allowed the energetic levels involved during light absorption and emission phenomena to be analyzed (Scheme S1 in the SI). Emission spectra with λ^{ex} = 350 nm on **1** at 80 K (Figure 3) present a major contribution (λ_{max} = 394 nm) attributed to the radiative de-excitation of the excited enol* form (pathway A in Scheme S1). At a higher temperature, a significant bathochromic shift of ∼20 nm in this emission band was observed (λ_{max} = 414 nm at 259 K) along with a second band at $\lambda_{max} \approx$ 510 nm attributed to

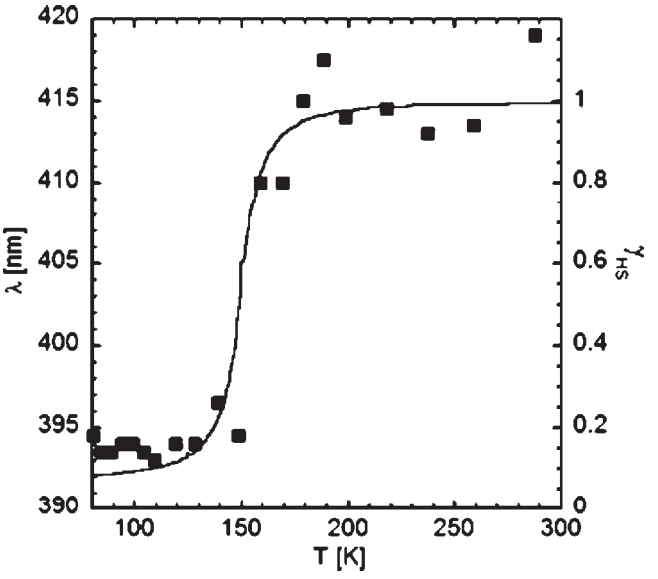

Figure 4. Temperature dependence of λ_{max} enol* in the emission spectrum of **1** (■), which follows γ_{HS} derived from the SQUID data (solid line).

radiative relaxation of the excited *cis*-keto* form, which is produced through proton transfer in the excited state of the enol form of **L1** (pathway B in Scheme S1). These two emission bands were observed at λ_{max} = 444 and 526 nm for **L1** (λ_{ex} = 350 nm, 80−289 K), indicating a major impact of the coordination of iron ions (Figure S3c).

Emission spectra of **1** were also recorded at λ_{ex} = 400 nm (80 K) and revealed a broad band at λ_{max} = 461 nm attributed to the radiative relaxation of the *cis*-keto* form (Figure S3b). For **L1**, a broad band was also noticed at ∼493 nm at 80 K (Figure S3d) with more than four nonresolved contributions attributed to several molecular conformations.[17] An increase in temperature revealed a band at higher wavelength attributed to the emission from a more stable and relaxed conformation of the *cis*-keto form in **L1**, as discussed for *N*-(5-chloro-2-hydroxybenzylidene)aniline.[17]

We selected the temperature shift of the wavelength emission maximum of the enol* band (λ_{max} enol*) as a marker to determine whether the SCO event could be tracked by fluorescence. As shown in Figure 3, a drastic jump of 20 nm was observed over the temperature range 135−179 K, from ∼395 nm below 150 K to 415 nm above 200 K. Remarkably, such a dramatic increase in the wavelength precisely follows the temperature dependence of the HS molar fraction (γ_{HS}) derived by SQUID measurements (Figure 4). Thus, fluorimetry was successfully used to track a SCO in an iron(II) complex in the crystalline state directly for the first time. The transition temperature, $T_{1/2}$ = 157(1) K, is in good agreement with the one obtained by DSC [T_{max} = 155(1) K]. In contrast to **1**, the variable-temperature study of λ_{max} enol* for **L1** showed only a slow decrease of ∼9 nm, presumably due to a slight change in the strength of the supramolecular interactions induced by the temperature change (Figure S4b).

Similarly, the SCO curve for **1** could be tracked by following the temperature dependence of the wavelength emission maximum of the *cis*-keto* band (λ_{max} cis*). Indeed, a drastic modification around $T_{1/2}$ was observed, in contrast to the almost stable emission wavelength observed for **L1** (Figure S5). Interestingly, the fluorescence enhancement observed below $T_{1/2}$ (Figure 3) can be related to the increase of rigidity of the lattice as the ST proceeds to the LS state.

In summary, we have presented the crystal structures of a thermochromic dinuclear iron(II) complex bridged by three *N*1,*N*2-1,2,4-triazole ligands in both its HS and LS states. This dinuclear unit, which was known only within a pentanuclear assembly in the HS state,[18] can be considered as a suitable structural model of the 1D 1,2,4-triazole iron(II) coordination polymers[13] that have been intensively studied as promising switches for spintronics and magnetic device fabrication[19,20] and whose crystal structure is still awaited.[21] The abrupt change in the magnetic properties of **1** results from the cooperative manifestation of the ST process thanks to intra- and intermolecular interactions mediated by 1,2,4-triazole and supramolecular interactions, respectively. This one-component system presents fluorescence properties linked to an intraligand electronic transition that allow tracking of the ST curve in good agreement with other physical methods. This analytical tool opens up an avenue for probing techniques to track thermosensitive events in multifunctional magnetic materials. This complex affords an unique platform for future photomagnetic studies, namely, the light-induced excited-spin-state trapping (LIESST) and ligand-driven light-induced spin change (LD-LISC) effects,[22] the latter being potentially accessible through the formation of the *trans*-keto form of the *N*-salicylidene ligand.[15]

■ ASSOCIATED CONTENT

Supporting Information. Experimental details for the synthesis of **1**; crystallographic data for **1** in the HS and the LS states, including CIFs; photochemical pathways in the emission spectrum; ^{57}Fe Mossbauer spectra and data (77−300 K), diffuse reflectance spectra for **L1** and **1**; and temperature-dependent emission spectra for **L1** and **1**. This material is available free of charge via the Internet at http://pubs.acs.org. Crystallographic data can be obtained free of charge from the Cambridge Crystallographic Data Center via www.ccdc.cam.ac.uk/data_request/cif.

■ AUTHOR INFORMATION

Corresponding Author
yann.garcia@uclouvain.be

■ ACKNOWLEDGMENT

This work was partially funded by the Fonds de la Recherche Scientifique-FNRS (FRFC 2.4508.08, IISN 4.4507.10), the IAP-VI (P6/17) INANOMAT Program, and the Concerted Research Action of the "Communauté Française de Belgique" from the Académie Universitaire Louvain. We thank the Fonds pour la Formation à la Recherche dans l'Industrie et dans l'Agriculture for a doctoral scholarship allocated to F.R.

■ REFERENCES

(1) (a) Gütlich, P.; Garcia, Y.; Spiering, H. *Magnetism: From Molecules to Materials*; Wiley-VCH: Weinheim, Germany, 2003; pp 271−344. (b) Gütlich, P.; Garcia, Y.; Goodwin, H. A. *Chem. Soc. Rev.* **2000**, *29*, 419. (c) Venkataramani, S.; Jana, U.; Dommaschk, M.; Sonnichsen, F. D.; Tuczek, F.; Herges, R. *Science* **2011**, *331*, 445.

(2) Brooker, S.; Kitchen, J. A. *Dalton Trans.* **2009**, 7331.

(3) Lilly, G. D.; Whalley, A. C.; Grunder, S.; Valente, C.; Frederick, M. T.; Stoddart, J. F.; Weiss, E. A. *J. Mater. Chem.* **2011**, *21*, 11492.

(4) Chong, C.; Mishra, H.; Boukheddaden, K.; Denise, S.; Collet, E.; Ameline, J.-C.; Naik, A. D.; Garcia, Y.; Varret, F. *J. Phys. Chem. B* **2010**, *114*, 1975.
(5) Chong, C.; Berini, B.; Boukheddaden, K.; Codjovi, E.; Linares, J.; Garcia, Y.; Naik, A. D.; Varret, F. *Phys. Status Solidi A* **2010**, *207*, 1227.
(6) Coronado, E.; Galán-Mascarós, J. R.; Monrabal-Capilla, M.; García-Martínez, J.; Pardo-Ibáñez, P. *Adv. Mater.* **2007**, *19*, 1359.
(7) Alam, M. S.; Stocker, M.; Gieb, K.; Müller, P.; Haryono, M.; Student, K.; Grohmann, A. *Angew. Chem., Int. Ed.* **2010**, *49*, 1159.
(8) Boukheddaden, K.; Loutete-Dangui, E. D.; Koubaa, M.; Eypert, C. *Phys. Status Solidi C* **2008**, *5*, 1003.
(9) Naik, A. D.; Stappers, L.; Snauwaert, J.; Fransaer, J.; Garcia, Y. *Small* **2010**, *6*, 2842.
(10) (a) Edder, C.; Piguet, C.; Bünzli, J. C. G.; Hopfgartner, G. *Chem.—Eur. J.* **2001**, *7*, 3014. (b) Hasegawa, M.; Renz, F.; Hara, T.; Kichuki, Y.; Fukada, Y.; Okubo, J.; Hoshi, T.; Linert, W. *Chem. Phys.* **2002**, *277*, 21. (c) Matsuda, M.; Isozaki, H.; Tajima, H. *Chem. Lett.* **2008**, *37*, 374. (d) Tovee, C. A.; Kilnet, C. A.; Thomas, J. A.; Halcrow, M. A. *CrystEngComm* **2009**, *11*, 2069. (e) Engeser, M.; Fabbrizzi, L.; Licchelli, M.; Sacchi, D. *Chem. Commun.* **1999**, 1191.
(11) Salmon, L.; Molnár, G.; Zitouni, D.; Quintero, C.; Bergaud, C.; Micheau, J.-C.; Bousseksou, A. *J. Mater. Chem.* **2010**, *20*, 5499.
(12) Titos-Padilla, S.; Herrera, J. M.; Chen, X.-W.; Delgado, J. J.; Colacio, E. *Angew. Chem., Int. Ed.* **2011**, *50*, 3290.
(13) Garcia, Y.; Niel, V.; Muñoz, M. C.; Real, J. A. *Top. Curr. Chem.* **2004**, *233*, 229.
(14) Robert, F.; Naik, A. D.; Tinant, B.; Robiette, R.; Garcia, Y. *Chem.—Eur. J.* **2009**, *15*, 4327.
(15) Robert, F.; Naik, A. D.; Hidara, F.; Tinant, B.; Robiette, R.; Wouters, J.; Garcia, Y. *Eur. J. Org. Chem.* **2010**, 621.
(16) Hadjoudis, E.; Mavridis, I. M. *Chem. Soc. Rev.* **2004**, *33*, 579.
(17) Harada, J.; Fujiwara, T.; Ogawa, K. *J. Am. Chem. Soc.* **2007**, *129*, 16216.
(18) Kolnaar, J. J. A.; de Heer, M. I.; Kooijman, H.; Spek, A. L.; Schmitt, G.; Ksenofontov, V.; Gütlich, P.; Haasnoot, J. G.; Reedijk, J. *Eur. J. Inorg. Chem.* **1999**, 881.
(19) Kahn, O.; Martinez, C. J. *Science* **1998**, *279*, 44.
(20) Prins, F.; Monrabal-Capilla, M.; Osorio, E. A.; Coronado, E.; van der Zant, H. S. J. *Adv. Mater.* **2011**, *23*, 1545.
(21) Dîrtu, M. M.; Neuhausen, C.; Naik, A. D.; Rotaru, A.; Spinu, L.; Garcia, Y. *Inorg. Chem.* **2010**, *49*, 5723.
(22) Gütlich, P.; Garcia, Y.; Woike, Th. *Coord. Chem. Rev.* **2001**, *219–221*, 839.